Numerical analyses of human body impact to parameters of wearable antenna under deformations

*Note: Sub-titles should not be used

Jugoslav Jokovic
Faculty of Electronic Engineering, University of Niš, Serbia
jugoslav.jokovic@elfak.ni.ac.rs & ORCID 0000-0002-4780-938X

Aleksandar Atanaskovic
Faculty of Electronic Engineering, University of Niš, Serbia
aleksandar.atanaskovic@elfak.ni.ac.rs &
ORCID 0000-0002-9979-5995

Tijana Dimitrijevic
Faculty of Electronic Engineering, University of Niš, Serbia
Faculty of Engineering, University of Kragujevac, Serbia
tijana.dimitrijevic@elfak.ni.ac.rs & ORCID 0000-0002-9744-8287

Nebojša Dončov
Faculty of Electronic Engineering
University of Niš, Serbia
nebojsa.doncov@elfak.ni.ac.rs & ORCID 0000-0002-9057-6737

***Abstract*—This paper investigates the impact of the human body on impedance matching of wearable microstrip antennas under bending conditions. A cylindrical 3-D Transmission Line Matrix (TLM) in-house solver with conformal mesh is used for parametric analysis, enabling accurate modeling of curved geometries and antenna–body interaction. The study focuses on separating body-induced effects on reflection coefficient and resonant frequency from bending deformation and related mechanisms such as patch elongation and substrate permittivity variation. Results show that body loading significantly degrades impedance matching, while bending can partially reduce this effect by decreasing electromagnetic coupling with tissue. The proposed approach provides an efficient and physically consistent framework for predicting antenna performance in realistic wearable environments.**

Keywords—Wearable antennas, impedance matching, cylindrical TLM, bending, body loading, conformal modeling.

I. Introduction

Wearable antennas are fundamental components of Wireless Body-Centric Communication Systems (WBCCS), enabling applications in healthcare monitoring, biomedical sensing, sports analytics, military systems, and rescue operations [1-3]. The microstrip patch antennas are typically integrated into clothing or placed directly on the human body, requiring compact, lightweight, and conformal designs capable of maintaining stable electromagnetic performance under realistic operating conditions. Accurate prediction of antenna parameters is essential for ensuring stable performance in wearable environments related to geometrical deformations caused by body shapes and motions, as well as antena-body interactions in electromagnetic sense [1-9].

Extensive studies have investigated wearable antennas in both off-body and on-body configurations illustrating that wearable antenna resonance behavior under bending differs significantly. In the off-body bent antennas, frequency shifts are primarily caused by changes in effective electrical length of patch, fringing-field redistribution, and curvature-induced modification of current distribution. Unlike free-space operation, the proximity of biological tissue characterized by high permittivity and significant losses introduces strong electromagnetic loading. This interaction affects both the resonant frequency and impedance matching, often leading to frequency detuning and degradation of the reflection coefficient S11. Several studies reported that body additionally influences the resonance behavior of wearable antennas and often masks purely geometrical bending effects [8], while some experimental investigations also demonstrate that strongly bent antennas may exhibit partial recovery of impedance matching because increased curvature locally reduces electromagnetic coupling with tissue [9].

Generally, the effects of geometrical deformation and body loading in the most reported works are not clearly separated, making it difficult to quantify their individual contributions. Additionally, bending deformation introduces multiple coupled electromechanical effects, including patch elongation, substrate thickness reduction, and strain-dependent variations of permittivity and conductivity. These mechanisms can produce resonant frequency shifts and impedance changes that may either reinforce or counteract deformation and body-induced effects. Consequently, the observed resonance variation under bending represents a superposition of multiple mechanisms including geometrical deformation, body loading, and deformation induced electromechanical variation of flexible substrate and conductive materials. As a result, the observed variations in resonant frequency and S11 represent a superposition of body loading and deformation-driven phenomena, which are often treated jointly in simulations and experiments without clear distinction.

To address this limitation, this paper focuses on the separate quantification of human body impact on impedance matching and resonant frequency, distinguishing it from other electromechanical deformation-induced effects. In contrast to non-conformal discretization techniques, the approach based on cylindrical conformal TLM method [10–13] preserves field continuity and current distribution under bending, allowing reliable separation of body-loading effects from deformation-induced electromechanical variations. The analysis is based on a systematic comparison between off-body and on-body configurations, combined with controlled parametric studies of bending deformation along with strain induced efects.

ISBN 978-86-6200-074-3 ©2026 AM & ETRAN
https://doi.org/10.69994/13Ic26024

II. ANTENNA MODEL

The proposed cylindrical three-dimensional Transmission Line Matrix (3D-TLM) conformal solver [10–13], was employed to investigate the impact of human-body loading and bending deformation on the impedance matching characteristics of wearable microstrip antennas.

The analyzed structure presented in Figure 1 is a rectangular microstrip patch antenna operating in the 2.4 GHz ISM band, following the baseline configuration [11–13], consisting of:
- patch, with length $l = 39.5$ mm and width $w = 50$ mm;
- ground plane, with dimensions $L = W = 100$ mm;
- substrate, with relative permittivity $\varepsilon_r = 2.1 - j0.001$ and height $h = 2$ mm.

The microstrip antenna is fed by a coaxial probe positioned at $l_0 = 11.5$ mm from the radiating patch edge for impedance matching The antenna is analyzed in off-body (free space) and on-body mode, considering that is placed above a muscle-equivalent tissue layer with relative permittivity $52.67 - j13$, and the thickness of $d = 35$ mm [11, 13].

The in-house solver based on the cylindrical TLM method [10–13] is used for an electromagnetic analysis of E-plane bending, employing a conformal orthogonal polar grid in the *r-φ* plane, capable to consider different scenarios of bending and stretching effects, as presented in Figure 2. In this TLM formulation, bending deformation is modeled by wrapping the antenna over a part of cylinder which radius R determines bending angle as $2\theta = l / (R+h)$, considering patch as nonstretchable [11, 12]. The model of bent antenna [13] is extended by incorporating mechanical substrate height reduction, which also directly modifies electromagnetic behavior of the antenna, together with patch elongation and permittivity variation. For uniaxial tensile strain applied along the patch length, the substrate is exposed transverse contraction governed by Poisson's ratio ν, typically ranging from 0.3–0.5 for polymeric and textile substrates [7, 14]. Consequently, the substrate thickness decreases according to

$$h - \Delta h = h \times (1 - \nu \times f) \quad (1)$$

where f represents the effective strain of the textile substrate forming the air–fiber composite structure:

$$f = 1 / (1 + \Delta L/L) \quad (2)$$

Mesh discretization in the *φ*- direction that ensures correct modelling of the patch length under bending in E-plane, when patch elongation (Δl) and substrate height reduction (Δh) are simultaneously included, is defined through:

$$2\theta = (l + \Delta l) / (R + h - \Delta h) = \Delta\theta_{patch} \times N_{cells}(patch) \quad (3)$$

where $N_{cells}(patch)$ is a number of cells corresponding to the length of radiated patch l. With the patch elongation Δl and substrate height reduction Δh, cylindrical TLM modeling must slightly update angular discretization $\Delta\theta_{patch}$, in respect to these parameters related to bending induced strain. In order to preserve geometric conformity, considering ground plane as solid and nonstretchable in terms of elongation, the mesh resolution must be defined as

$$L / R = \Delta\theta_{patch} \times N_{cells}(patch) + \Delta\theta_{sub} \times N_{cells}(sub) \quad (4)$$

where $N_{cells}(sub)$ is a number of cells corresponding to the length of substrate $(L+\Delta L)$ excluding patch $(l+\Delta l)$. For fully stretchable materials the bending induced patch elongation ratio $\Delta l/l$ is equal to $\Delta L/L$ and can be determined through

$$(L + \Delta L) / (R + h - \Delta h) = L / R \quad (5)$$

The bent antenna model [13] also considers permittivity variation via the volume fraction permittivity (VFP) approach applied to air-solid mixture structure [15].

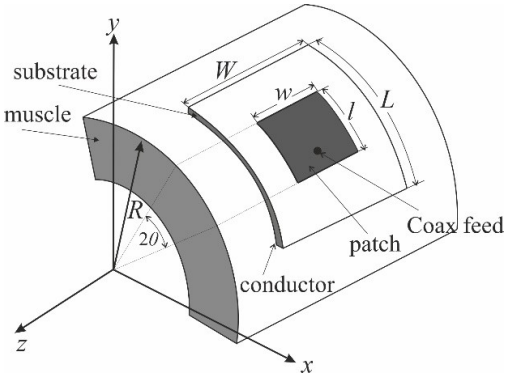

Fig. 1. A rectangular patch antenna with a bending 2θ in an E-plane [11].

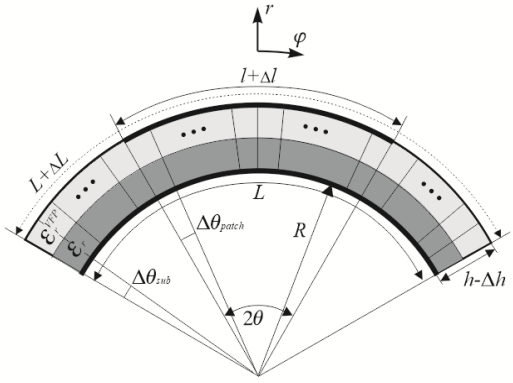

Fig. 2. Conformal orthogonal polar grid in the r-φ plane of antenna model (air padding and muscle layer are not presented)

Descriptor of the permittivity variation due to stretching is based on the substrate multilayered representation [13]. Depending on bending-induced strain permittivity of each layer can be determined according to formulas based on VFP [15]. Considering the permittivity of the bottom layer of the substrate placed on the nonstretchable ground plane ε_r, the permittivity of the upper layer of the substrate in the antenna model is calculated from [15] as

$$\varepsilon_r^{VFP} = \varepsilon_r / (f + (1 - f) \times \varepsilon_r), \quad (6)$$

Including the mechanical substrate height reduction via the Poisson's ratio ν, model is modified with slightly update radial discretization of upper substrate layer, from $h/2$ to $h/2-\Delta h$. In order to illustrate effect of thickness reduction, the Poisson's ratio value of 0.5, is chosen here, that is equivalent to incompressible elastomers [7, 14].

Table 1 presents computational mesh parameters, specifically cell size and the number of cells divided by axis relevant to a cylindrical coordinate system, which are used for modeling of patch antennas in free space and on a muscle

tissue. Since the patch antenna is considered as an open problem, an appropriate extension around the physical antenna structure is included to form a computational box (represented as air in the Table 1) allowing for the adequate representation of the antenna surroundings, necessary for the proper capturing of radiation and calculation of the antenna parameters. In the on-body case, the air region bellow the antenna is replaced with a tissue equivalent layer characterized by permittivity of muscle.

TABLE I. THE MESH PARAMETERS IN CYLINDRICAL TLM MODEL OF WEARABLE ANTENNA IN OFF-BODY AND ON-BODY CONFIGURATIONS

Axis	Medium/ Region	Permittivitty	Number of cells	Resolution/ Cell size
r-axis (height)	air/ muscle	1/ 52.67-*j*13	25/ 175	1.45mm/ 0.2 mm
	substrate	2.1-*j*0.001	2	1 mm
	air	1	28	1.45 mm
φ-axis (length)	air	1	28	$(R+h)\Delta\theta_{padd}$ =1.45 mm
	Substrate/ patch	2.1-*j*0.001	99	$\Delta\theta_{sub}=((L/R - l/(R+h))/60$, $R\Delta\theta_{sub}$=1.01 mm $\Delta\theta_{patch}=(l/(R+h))/39$, $(R+h)\Delta\theta_{patch}$=1.01 mm
	air	1	28	$(R+h)\Delta\theta_{padd}$ =1.45 mm
z-axis (width)	air	1	28	1.45 mm
	Substrate/ patch	2.1-*j*0.001	99	1 mm -1.02 mm
	air	1	28	1.45 mm

III. SIMULATION RESULTS

Figure 3 presents the reflection coefficient characteristics obtained using the proposed cylindrical 3-D TLM conformal solver summarize the parametric analysis of wearable antenna behavior under bending deformation for both off-body and on-body configurations. The curves compare the baseline bending effect with additional strain-induced mechanisms including patch elongation and substrate permittivity variation along with thickness reduction. The results demonstrate that body loading significantly modifies the resonance behavior and reduces the sensitivity of the antenna to bending-induced impedance perturbations. Initially, the antenna performance was analyzed in the flat configuration. In the off-body case, the antenna resonates at 2.444 GHz with optimized impedance matching and a reflection coefficient close to −40 dB. After placing the antenna on the human-body phantom, the resonant frequency remains nearly unchanged, while the reflection coefficient degrades to approximately -27 dB. These results confirm that the human body loading modifies the antenna input impedance and reduces resonance sharpness because of increased electromagnetic losses.

Figure 4 summarizes the variation of the minimum reflection coefficient level as a function of bending angle. The comparison separately quantifies the influence of pure bending, patch elongation, and substrate permittivity variation for both off-body and on-body cases. The results show that the degradation of S11 under bending is more pronounced in the off-body configuration. Since the antenna is initially well matched in free space, even moderate geometrical perturbations result in significant changes of the reflection coefficient. By contrast, in the on-body case the lossy body environment and reduced electromagnetic antenna-body coupling under curvature partially compensate deformation-induced mismatch effects.

Figure 5 shows the corresponding resonant-frequency variations under deformation. The presented trends indicate how the frequency shift in the off-body configuration under bending is governed by geometrical deformation effects. On the other side, the on-body response is additionally influenced by curvature-dependent body loading. Therefore, the observed resonant-frequency variation results from a superposition of geometrical deformation effects and curvature-dependent body loading, resulting in a larger net frequency shifts caused by bending compared to the off-body case. Additional simulations were performed to quantify the influence of strain-induced patch elongation, substrate permittivity variation and thickness reduction. The results based on both off-body and on-body configuration show that patch elongation produces the dominant downward resonant-frequency shift due to increased effective electrical length. Substrate permittivity variation along with thickness reduction introduces additional upward frequency correction. The decomposition of these mechanisms confirms that body loading remains the constant factor affecting impedance matching and resonance behavior, whereas electromechanical deformation mechanisms contribute to resonance detuning on the same manner in off-body an on body case.

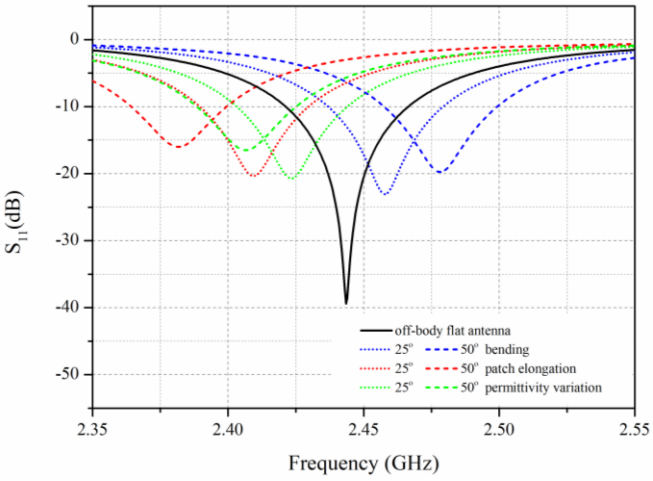

a)

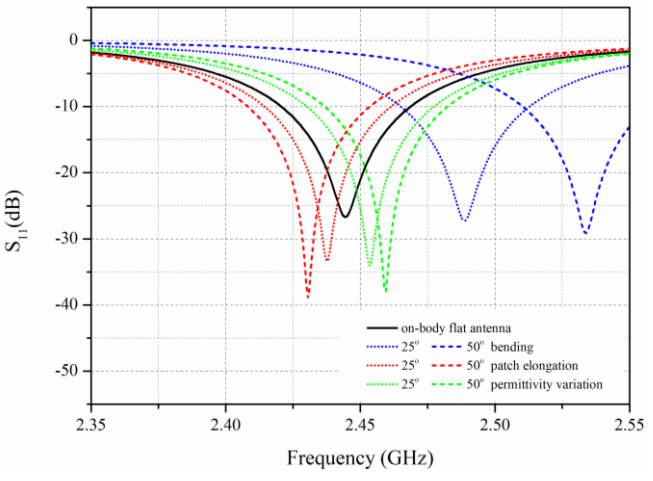

b)

Fig. 3. Reflection coeficient of wearable antenna under deffomations, for configurations: a) off-body, b) on-body

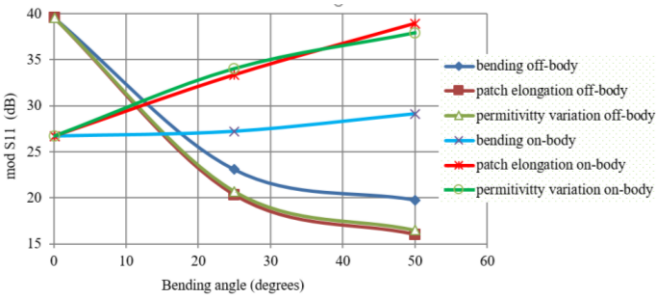

Fig. 4. Refflection coefficient level changes under deformations

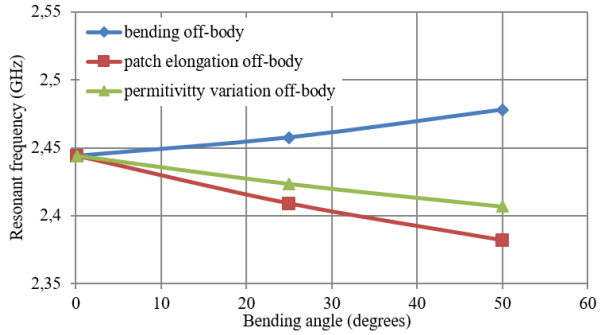

a)

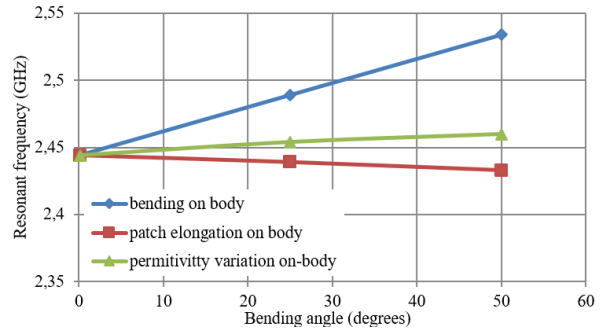

b)

Fig. 5. Resonant frequencies changes under deformations, , for configurations: a) off-body, b) on-body

IV. Conclussions

The presented results demonstrate that accurate wearable antenna characterization cannot rely solely on free-space analysis and simplified geometric bending models. The electromagnetic interaction with the human body significantly alters the impedance behavior and modifies the sensitivity of the antenna to bending deformation.

By establishing a clear separation between body loading and deformation effects, the presented framework provides improved physical insight into the mechanisms governing wearable antenna performance. This distinction is essential for accurate modeling, reliable parameter prediction, and the design of robust antennas capable of maintaining stable operation in dynamic body-centric environments. The cylindrical conformal TLM approach enables isolation of the body-induced contribution to S11 degradation and frequency detuning, while independently evaluating the influence of curvature-related structural changes. The developed framework therefore provides a computationally efficient and physically accurate tool for parametric studies of wearable antennas operating under realistic body-centric conditions..

Acknowledgment

This research was supported by the Science Fund of the Republic of Serbia, #GRANT No 377, Customized Models for Flexible Antennas Design - Custom-FlexMADE, and by the Ministry of Education, Science and Technological Development of Republic of Serbia (Grant number 451-03-34/2026-03/200102).

References

[1] U. Ali, S. Ullah, B. Kamal, L. Matekovits and A. Altaf, "Design, Analysis and Applications of Wearable Antennas: A Review", IEEE Access, vol. 11, pp. 14458-14486, 2023.

[2] V. Marterer, M. Radouchová, R. Soukup, S. Hipp and T. Blecha, "Wearable textile antennas: investigation on material variants, fabrication methods, design and application", *Fashion and Textiles*, vol. 11, no.9, 2024.

[3] F.F. Hashim, W.N.L.B. Mahadi, T.B. Al Latef, and M. B. Othman, "Key Factors in the Implementation of Wearable Antennas for WBNs and ISM Applications: A Review WBNs and ISM Applications: A Review", *Electronics,* vol. 11, no. 15: 2470, 2022.

[4] Hertleer, C., Rogier, H., Vallozzi, L. and Van Langenhove, L. (2009) A Textile Antenna for Off-Body Communication Integrated into Protective Clothing for Firefighters. IEEE Transactions on Antennas and Propagation, 57, 919-925.

[5] L. Vallozzi, H. Rogier, C. Hertleer, and L. Van Langenhove,"Wearable Textile Antennas," IEEE Antennas and Propagation Magazine, vol. 55, no. 2, pp. 63–73, Apr. 2013

[6] I. Locher, M. Klemm, G. Troster, "Design and Characterization of Purely Textile Patch Antennas", *IEEE Trans. on Adv. Packaging,* vol. 29, no. 4, pp.777-788, 2006..

[7] R. Salvado, C. Loss, R. Gonçalves and P. Pinho, "Textile Materials for the Design of Wearable Antennas: A Survey", *Sensors* 2012, vol.12, no.11, pp.15841-15857, Nov. 2012.

[8] P. Salonen and Y. Rahmat-Samii, "Textile Antennas: Effects of Antenna Bending on Input Matching and Impedance Bandwidth," in *Proc. IEEE Antennas and Propagation Society Int. Symp.*, Honolulu, HI, USA, 2007, pp. 1–4.

[9] S. Zhu and R. Langley, "Dual-Band Wearable Textile Antenna on an EBG Substrate," *IEEE Transactions on Antennas and Propagation*, vol. 57, no. 4, pp. 926–935, Apr. 2009

[10] T. Dimitrijevic, J. Jokovic, N. Doncov, "Efficient Modelling of a Circular Patch-Ring Antenna Using the Cylindrical TLM Approach", *IEEE Antennas and Wireless Propagation Letters*, vol.16, pp. 2070-2073, April 2017.

[11] J. Jokovic, T. Dimitrijevic, A. Atanaskovic, and N. Doncov, "Computational Modeling of the Bent Antenna in an On-Body Mode Using the Cylindrical TLM Approach", *Math. Probl. Engineer.*, vol. 2022, Article ID 8486740, 2022.

[12] T. Dimitrijevic, A. Vukovic, A. Atanaskovic, J. Jokovic, P. Sewell, and N. Doncov, "Holistic Analysis of Conformal Antennas Using the Cylindrical TLM Method", *IEEE Trans. Ant. Prop.*, vol. 71, no. 5, pp. 4028 – 4035, 2023.

[13] J. Jokovic, T. Dimitrijevic, A. Atanaskovic, and N. Doncov, "Modelling of Textile Patch Antenna Deformations by the Cylindrical TLM Method", *IEEE TELSIKS Conference,* Nis, Serbia, pp. 266-269, October 2025.

[14] F. P. Beer, E. R. Johnston, J. DeWolf, and D. Mazurek, *Mechanics of Materials*, McGraw-Hill, 7th edition, 2015.

[15] K. Bal and V.K. Kothari, "Permittivity of Woven Fabrics: A comparison of Dielectric Formulas For Air-Fiber Mixture", *IEEE Trans. on Dielectrics and Electrical Insulation* vol. 17. no. 3, pp.881 – 889, July 2010.